Microgel-Based Etalon Coated Quartz Crystal Microbalances for Detecting Solution pH: The Effect of Au Overlayer Thickness

Molla R. Islam, Kai C.C. Johnson and Michael J. Serpe*

Department of Chemistry, University of Alberta, Edmonton, AB, T6G 2G2 (Canada)
E-mail: michael.serpe@ualberta.ca

Keywords: Poly (*N*-isopropylacrylamide)-based microgels, Quartz crystal microbalance, Microgel-based etalons, pH sensing.

Abstract:

Poly (*N*-isopropylacrylamide)-*co*-acrylic acid (pNIPAm-co-AAc) microgels were "painted" on the Au electrode of a quartz crystal microbalance (QCM). Another Au layer (overlayer) was subsequently deposited on the microgel layer. This structure is known as a microgel-based etalon. These devices have been shown to exhibit optical properties (i.e., color) that depend on solution pH and temperature, among other things. Previously, we measured QCM frequency shifts that are a result of solution pH changes; the frequency shifts are a direct result of the pH dependent solvation state of the microgels that make up the etalon. In fact, the shifts observed for the etalons were much greater in magnitude than just a microgel layer immobilized on the QCM crystal without the Au overlayer. We reasoned that the Au overlayer lead to an enhancement of the observed frequency change due to its mass. In this submission we investigate how the Au overlayer thickness (mass) affects the observed sensitivity to solution pH. We found that the change in QCM resonant frequency depended dramatically on the mass of the Au overlayer.

1. Introduction:

Stimuli responsive materials are capable of responding to changes in their environment by changing their conformation, chemistry, and/or molecular weight (among other things). In most cases, the response is reversible, i.e., when the stimulus is removed, the responsive material returns to its original state before the stimulus was applied [1-4]. These responsive materials can be composed of small molecules to polymeric systems including gels, composites and self-assembled aggregates [5-10]. Most commonly, stimuli responsive materials respond to changes in solution pH, temperature, and/or ionic strength [11-13]. Other materials have been developed that are responsive to specific analytes [14, 15], electrochemistry [16, 17], mechanical force [18, 19], electric or magnetic fields [20, 21] and light [22-23]. Responsive materials have found their way in a number of applications like chromatography [24, 25], optoelectronics [26, 27], drug delivery and biosensors [28, 29].

Of the responsive materials, polymer-based materials are the most common due to their ease of synthesis and chemical versatility. There are number of polymeric systems which respond to specific and unique stimuli, but poly(*N*-isopropylacrylamide) (pNIPAm) is the most widely studied. PNIPAm is a thermoresponsive polymer, which undergoes a volume phase transition at ~32 °C, which is pNIPAm's lower critical solution temperature (LCST) [30,31]. That is, pNIPAm is water-soluble at T < 32 °C, existing as a water solvated, random coil. At T > 32 °C, pNIPAm expels its solvating water and becomes insoluble, existing as a globule. Colloidally stable hydrogels, (microgels) can also be synthesized from pNIPAm. These crosslinked polymer networks are swollen with water (large diameter) at T < 32 °C, and dehydrate (small diameter) above that temperature. During that transition the microgels convert from a low viscosity state (swollen) to a high viscosity (deswollen) state [32,33].

PNIPAm-based microgels are very easily synthesized via free radical precipitation polymerization [34, 35]. The diameter of the microgels, as well as their chemical functionality, are very easily modified and tuned using this approach [36-38]. For example, comonomers can be easily added to the synthesis to render the microgels responsive to other stimuli, in addition to temperature. The most common comonomer is acrylic acid (AAc) [39, 40], which has a pK_a of ~ 4.25. Therefore, at pH > pK_a, the microgels are deprotonated, which renders the microgel network anionic; the microgels swell as a result of the Coulombic repulsion in the microgel network. The microgels return to their original diameter upon lowering the solution pH to < pK_a.

We have recently developed an optical device by sandwiching pNIPAm-based microgels between two thin Au layers [41-44], as shown schematically in Figure 1. We have shown that when these devices (etalons) are immersed in water, they exhibit visible color, and unique reflectance spectra, due to light interference in the cavity formed by microgel particles between the two Au layers. The specific color depends on the distance between the mirrors. Since the diameter of the microgels depends on temperature (and pH if AAc is present), the distance between the mirrors can be changed, and hence the etalon's color can be tuned dynamically [42-45].

In this submission we exploit the solvation state (and viscosity) changes that take place when an etalon changes color, as opposed to exploiting the actual color change, for sensing purposes. This is done by fabricating an etalon on the Au electrode of an AT-cut quartz crystal microbalance (QCM). An AT-cut QCM crystal can be excited electrically to undergo an oscillating shearing motion, at a characteristic resonant frequency (most commonly 5 MHz). The resonant frequency is dependent on the properties (e.g., mass, viscosity) of the material in contact with the oscillating device and is described by Eq.(1): [45].

$$\Delta f = -f_0^2(\eta_l \rho_l / \pi \rho_q \mu_q)^{1/2} \quad \text{.....(1)}$$

where f_0 is the initial resonant frequency of the QCM crystal, Δf is the frequency shift measured by the quartz crystal microbalance, ρ_l is the liquid density, η_l is the liquid viscosity, μ_q is the elastic modulus of quartz, and ρ_q is the density of quartz.

From equation (1), it can be see that the QCM resonant frequency decreases as the viscosity of the substance contacting the QCM crystal increases [45, 46]. Furthermore, increased viscosity leads to an increase in the "resistance" of QCM oscillation.

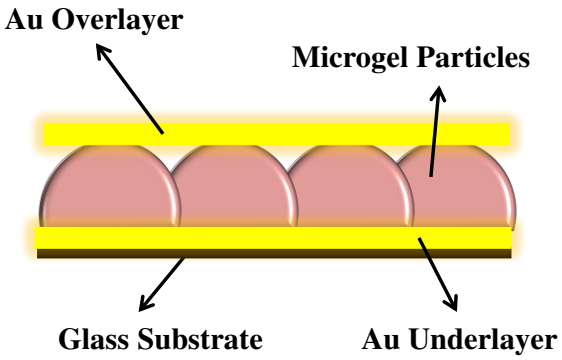

Figure 1: The basic structure of a microgel-based etalon. The Au overlayer in the figure is actually conformal to the microgel layer. There is a 2 nm Cr layer below the Au layers as an adhesion layer. The microgel layer is monolithic in nature. For this study, the "glass" is replaced with quartz.

We demonstrated that pNIPAm microgel-based etalons can be fabricated on the Au electrode of a quartz crystal microbalance (QCM) [33] and found that the resonant frequency of

a microgel coated QCM crystal and an etalon coated QCM crystal depended dramatically on the temperature and pH of the solution it was exposed to. We hypothesized that the behavior was a result of the microgels changing solvation state, and hence viscosity, under the various conditions. Specifically, at T > 32 °C and pH 3.0 the microgel are fully collapsed and have a high viscosity. When the solution pH is switched to 7.0, the microgels swell due to Coulombic repulsion in the microgel network, and their viscosity decreases. Therefore, the QCM resonant frequency transitions from a low to a relatively high frequency. In those investigations we observed that the QCM crystals coated with microgel-based *etalons* always exhibited greater frequency shifts than QCM crystals coated with microgels only (i.e., no Au overlayer). We attributed the enhanced response to the presence of the Au overlayer of the etalon interacting with the QCM crystal. For example, at high temperature and pH < pK_a, the Au overlayer of the etalon is close to the QCM crystal, and therefore its mass is "felt" by the QCM. In this case the microgel viscosity, in addition to the Au mass, is resulting in the observed QCM frequency. In contrast, the QCM crystals coated with only microgels only "feel" the microgel viscosity, therefore the initial resonant frequency isn't as low as what is observed for the etalon coated QCM crystal. In both cases, the microgels swell when the solution pH is switched to 7.0, and the QCM resonant frequency goes to approximately the same values. This is because the microgels are so swollen that the Au layer can no longer be "felt" by the QCM crystal, and hence the microgel viscosity dictates the QCM resonant frequency, which is approximately the same in both cases. We hypothesized that because the etalon coated QCM crystal started at a lower frequency (before the pH change), the *change* in frequency is much larger for the etalon coated QCM crystal. That is, the Au overlayer makes the device much more sensitive to pH.

Since we determined that the Au overlayer played a major role in the sensitivity of the QCM crystal to solution pH, we wanted to determine if changing the Au overlayer thickness (and hence mass) could enhance the response. That is, since we hypothesized that the enhanced response is due to the QCM crystal feeling the Au mass at high temperature and low pH, the response should be enhanced as the Au overlayer thickness is increased. In that case the QCM frequency should start off at lower frequencies with increasing Au overlayer thickness, and the observed shift on increasing the pH should be larger. In this submission, the QCM crystal's response to pH was investigated as a function of Au overlayer thickness, and it was found that the sensitivity of the device to solution pH increased with Au overlayer thickness.

2. Experimental

2.1. Materials

N-Isopropylacrylamide was purchased from TCI (Portland, Oregon) and purified by recrystallization from hexanes (ACS reagent grade, EMD, Gibbstown, NJ) prior to use. N,N′-methylenebisacrylamide (BIS) (99%), acrylic acid (AAc) (99%), and ammonium persulfate (APS) (98+%) were obtained from Sigma–Aldrich (Oakville, ON) and were used as received. Sodium chloride and sodium hydroxide were obtained from Fisher (Ottawa, ON). All deionized (DI) water was filtered to have a resistivity of 18.2 MΩ·cm and was obtained from a Milli-Q Plus system from Millipore (Billerica, MA). Cr and Au were deposited using a model THEUPG thermal evaporation system from Torr International Inc. (New Windsor, NY). Anhydrous ethanol was obtained from Commercial Alcohols (Brampton, ON). Hydrochloric acid was purchased from Caledon Chemicals (Georgetown, ON). Cr was 99.999% and obtained from ESPI as Cr

131 flakes (Ashland, OR), while Au was 99.99% and obtained from MRCS Canada as Au shot
132 (Edmonton, AB).

133 **2.2. Instrumentation**

134 Microgel coated QCM crystals, as well as the etalon coated devices were analyzed using
135 a QCM-200 obtained from Stanford Research Systems (Sunnyvale, CA). The crystal was placed
136 into a specially designed holder, which allowed for water of a given pH and temperature to
137 constantly flow over the crystal at a rate of 0.062 mL s^{-1}. This flow was maintained by a FMI lab
138 pump model RP-G150 (Oyster Bay, NY). The temperature was controlled by placing a beaker
139 containing water onto a Corning model PC-420D hotplate (Lowell, MA), and the water
140 temperature measured *via* a thermocouple. To change the pH of the solution, aliquots of either
141 1 M NaOH or concentrated HCl were added to the water, and the water pH measured with a
142 Jenco model 6173 pH meter (San Diego, CA). Ionic strength was not controlled, but we
143 confirmed that a change in ionic strength has a negligible effect on the resonant frequency of the
144 QCM crystal.

145 **2.3. Procedures**

146 **2.3.1. PNIPAm-co-AAc microgel synthesis**

147 The microgels used in this study were synthesized using surfactant-free, free radical
148 precipitation as described previously with NIPAm (85%), BIS (5%) and AAc (10%) [41-44].
149 Briefly, 8.5 mmol of NIPAm monomer and 0.51 mmol of N,N′-methylenebisacrylamide (BIS)
150 as the crosslinker was added to a beaker containing 50 mL of deionized water. The solution was
151 stirred by a magnetic stirrer for about 0.5 h. Once dissolved, the solution was filtered via a
152 syringe through a 0.2 μm syringe filter into a 100 mL 3-necked round bottom flask. 12.5 mL of

153 deionized water was used to rinse the beaker, which was also filtered and added to the round
154 bottom flask. Next, a gas inlet (needle), a reflux condenser, and a temperature probe were fitted
155 onto the round bottom flask. The solution was stirred at 450 RPM, and N_2 gas was purged
156 through the solution while heating to 45 °C for ~1 h. Bubbling N_2 gas into the solution was
157 stopped but continued to be introduced to keep the reaction atmosphere oxygen free.
158 Immediately prior to initiation, 1 mmol of AAc was added to the solution along with 2.5 mL of
159 0.078 M ammonium persulfate solution. The solution temperature was then increased to 65 °C at
160 a rate of 30 °C h^{-1}immediately following initiation and was allowed to react overnight.
161 Following the overnight reaction, the solution was allowed to cool and was filtered through glass
162 wool to remove large aggregates from the solution. The filtrate was then diluted to 120 mL with
163 deionized water and 12 mL aliquots were added to centrifuge tubes, and centrifuged at ~8500
164 relative centrifugal force for 30 min at 23 °C. The microgels were packed at the bottom of the
165 centrifuge tube, and the supernatant solution subsequently removed, and replaced with fresh DI
166 water. The packed microgels were loosen and vortexed to distribute the microgels into the water.
167 Centrifugation and resuspension was repeated five more times to remove any unreacted reagents,
168 linear polymers, and oligomers present with the microgel. After that pure, concentrated and very
169 viscous microgel pellet was formed and kept in the centrifuge tube for further use.

170 **2.3.2. Formation of etalons on QCM crystals**

171 The Au electrodes of the QCM crystals were rinsed copiously with anhydrous ethanol
172 and dried with N_2 gas. 25 μL of a concentrated, viscous microgel solution was “painted” only on
173 the “large” Au electrode of the QCM crystal and allowed to dry for 30 min at 35 °C [33]. All
174 experiments mentioned in this paper involve a QCM crystal painted with 25.0 μL of large
175 pNIPAm-co-AAc microgels. Following drying, the microgels not directly bound to the Au

electrode were rinsed off with DI water, and the QCM crystal was immersed in DI water overnight at 30 °C. Following soaking, the crystal was further rinsed with DI water and dried with N_2 gas. A paper template was adhered to the QCM crystal, such that only the large Au electrode, which was coated with microgels, was exposed. The QCM crystal was then inserted into a thermal evaporation system by Torr International Inc. (New Windsor, NY) model THEUPG. A thin layer of 2 nm Cr and the desired thickness of Au (15, 45, 60 and 200 nm) were deposited only onto the Au bound microgel layer at a rate of ~0.2 Å s^{-1} and ~0.1 Å s^{-1}, for Cr and Au, respectively. Here the Cr layer acts as adhesion layer for Au. After application of this overlayer, the crystal was removed from the vacuum chamber and immersed in DI water overnight at 30 °C. The QCM bound etalon was subsequently used.

3. Results and Discussion:

It is well known that increasing the temperature of a solution of pNIPAm-co-AAc microgels above the LCST in pH 3.0 solution causes them to collapse. If the pNIPAm-co-AAc microgels are deposited on the Au electrode of a QCM crystal, and undergo this transition, the resonant frequency of the crystal will decrease. This is a result of the microgels collapsing, and increasing viscosity, which yields a frequency decrease [33, 45]. In our previous studies, we determined that the minimum frequency is observed at the LCST for the microgels [33]. We found that the magnitude of the frequency shift, compared to its initial frequency, was much larger if Au was deposited on the microgel layer to make what is referred to as an etalon. As stated above, we hypothesize that the enhanced frequency response comes from the mass of the Au layer deposited on the microgels. We also determined that increasing the pH of the solution to 7.0 (at T > LCST) causes the microgels to swell due to Coulombic repulsion among the negatively charged acrylic acid groups that are formed in the microgel layer. This resulted in a

dramatic increase in the QCM resonant frequency due to the decrease in the viscosity of the etalon's microgel layer [33]. We have shown that the total frequency shift as a result of the pH change was much greater for the etalon, for reasons described above. In this submission we deposited Au layers of varying thicknesses onto the microgel layer deposited on the QCM's Au electrode. We hypothesize that the thicker Au overlayers will yield a device with enhanced pH sensitivity.

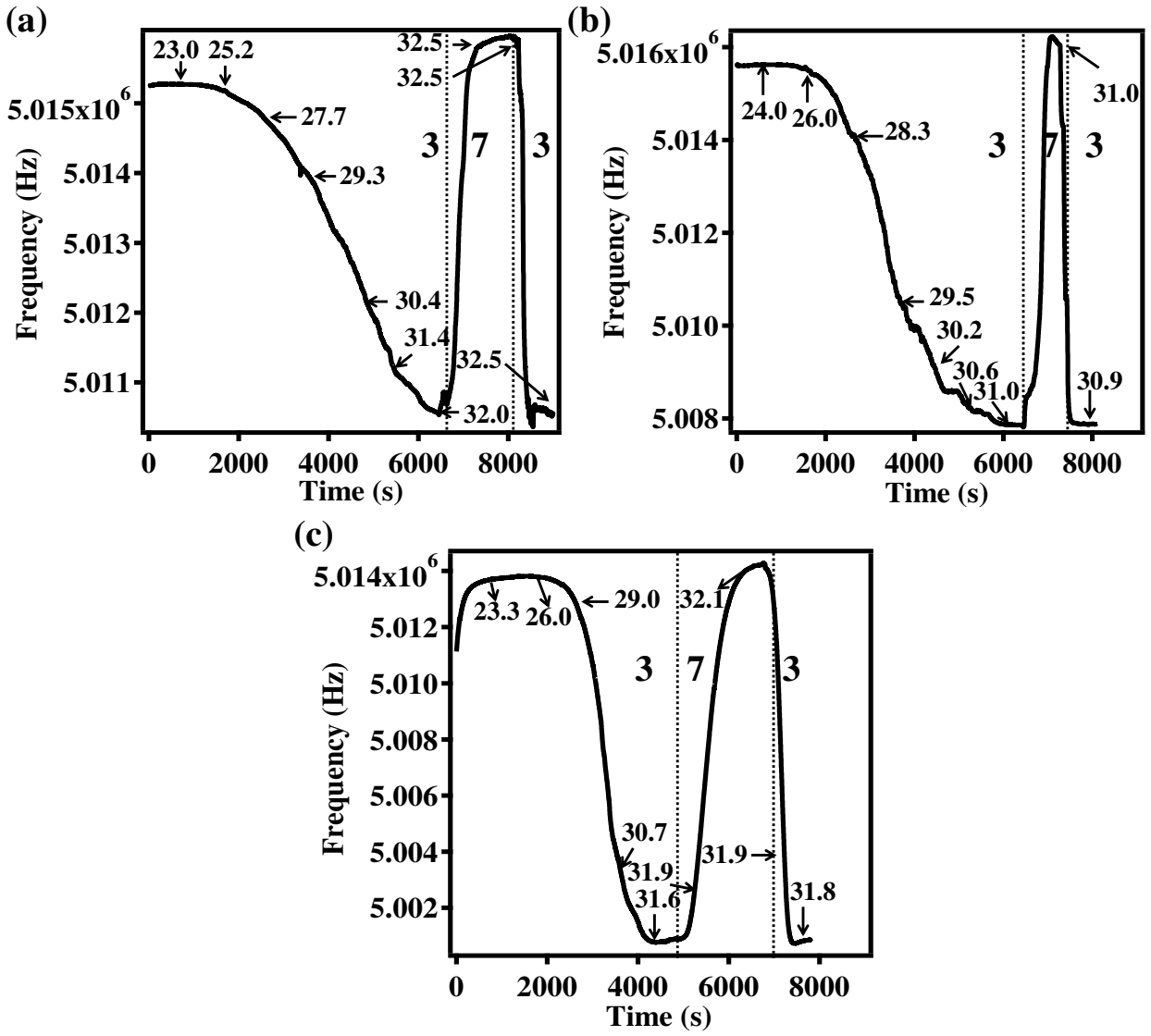

Figure 2: QCM resonant frequency as a function of time, temperature (values next to arrows), and pH for (a) an uncoated microgel layer on a QCM crystal, (b) a microgel layer coated with 15 nm of Au on a QCM crystal, and (c) a microgel layer coated with 45 nm of Au on a QCM crystal. The dashed lines indicate the time at which the pH was altered. The pH was increased using 1 M NaOH while the decrease in pH was achieved by adding increments of 12.1 M HCl.

Figure 2 shows the QCM crystal's response to temperature and pH for a QCM crystal that has its Au electrode painted with microgels, microgels with 15 nm of Au deposited, and 45 nm of Au deposited. The QCM device was placed in a pH 3.0 solution at room temperature and stabilized. Then the temperature of the solution was raised to the LCST of pNIPAm-co-AAc microgel (~32°C), and in each case the QCM resonant frequency decreased as a function of increasing temperature. A minimum resonant frequency is reached at ~ LCST, where the microgels are the most collapsed, and have the highest viscosity. We found that the extent of the frequency change with temperature increased for microgel layers coated with thicker (and heavier) Au overlayers. This can be seen in Figure 3. For example, we found frequency shift of ~15000 Hz for the 60 nm overlayer and ~32000 Hz for the 200 nm overlayer. We hypothesize that this trend of increased sensitivity with Au overlayer thickness is due to the enhanced Au mass the QCM felt at microgel's LCST. Once the frequency was stable at high temperature, the solution pH was elevated to 7.0 to enable the microgels to swell (and decrease viscosity) via Coulombic repulsion between the deprotonated acrylic acid groups in the microgel. It is interesting to note that the final frequency observed is relatively independent of Au overlayer thickness. In fact, when the difference between the QCM frequency at low temperature and pH 3.0 and high temperature at pH 7.0 is compared, there is a minimal dependence on Au overlayer thickness, as can be seen in

Figure 3. Therefore, in this system, it is the mass of the Au in the deswollen state that leads to enhanced sensitivity to pH. This is depicted in Figure 4, which shows the QCM's frequency response to pH. There is a nearly linear dependence on the frequency shift and Au overlayer thickness. In our previous publication we showed that the response occurred over a 2 pH unit range centered at AAc's pK_a [33]. Therefore, for the 200 nm Au overlayer we can achieve a sensitivity of 6.67 x 10^{-5} pH unit • Hz^{-1}. Based on the data in Figure 4, we hypothesize that the device's sensitivity could be enhanced by simply increasing the Au overlayer thickness. Upon stabilization of the QCM resonant frequency, the pH of the solution was returned to 3.0, leading to a concomitant return of the resonant frequency to its initial value. The change in pH from 7.0 to 3.0 at elevated temperature decreases the resonance frequency as the microgels deswell due to AAc protonation.

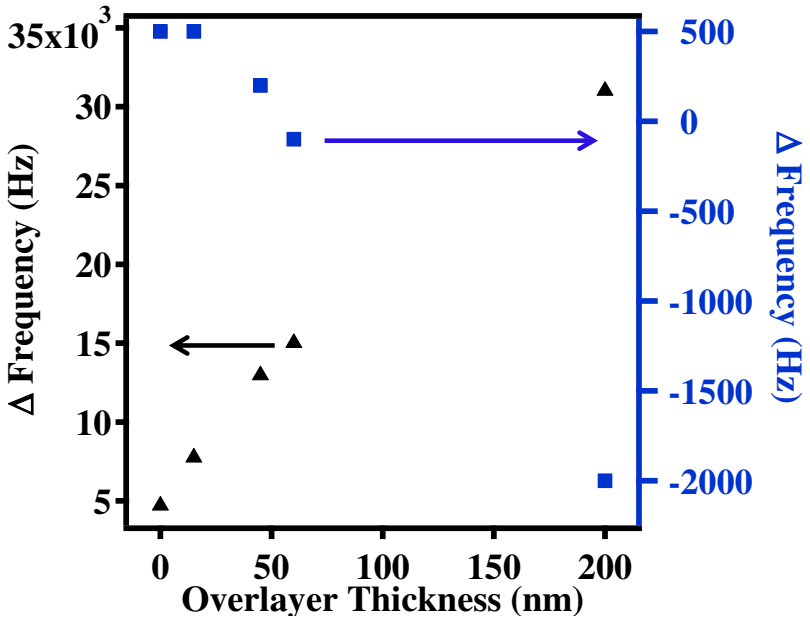

Figure 3: The observed QCM frequency changes for (▲) the temperature increase at pH 3.0, and (■) the difference between the etalons initial frequency at RT and pH 3.0 and its frequency at elevated temperature at pH 7.0. As can be seen, the Au overlayer thickness influences the QCM

frequency when the Au is close to the QCM surface, but has less of an influence on the frequency in the swollen state.

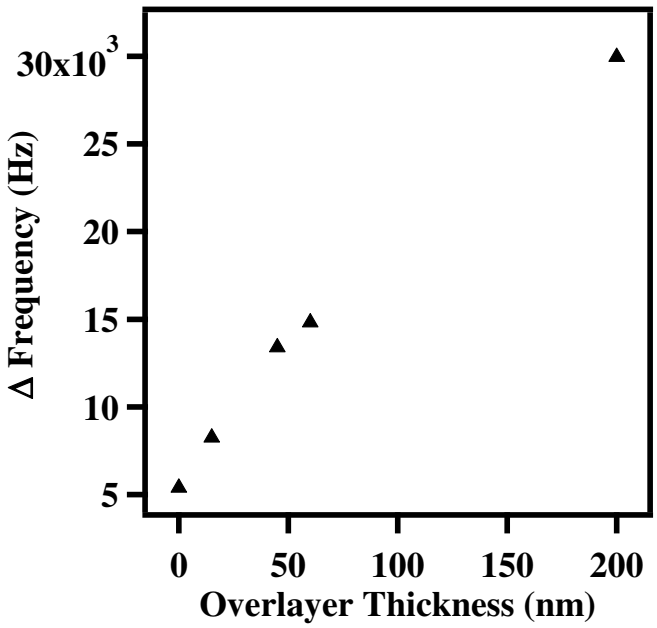

Figure 4: The influence of the Au overlayer thickness on QCM's response to the solution pH change.

4. Conclusion:

PNIPAm microgel-based etalons coated on the Au electrode of a QCM crystal was used to detect the temperature and pH of aqueous solutions. It was found that the QCM's response to pH depended dramatically on the thickness of the Au overlayer. Through analysis of our data, we determined that the increased Au thickness (mass) dramatically affected the QCM frequency at high temperature and pH 3.0, which leads to the enhanced response to pH for etalons composed of thick Au overlayers. This sensitivity of this system to solution pH can be extended to detect other analytes in solution, e.g., proteins and DNA that are indicative of disease.

Acknowledgements:

MJS acknowledges funding from the University of Alberta (the Department of Chemistry and the Faculty of Science), the Natural Science and Engineering Research Council (NSERC), the Canada Foundation for Innovation (CFI), the Alberta Advanced Education & Technology Small Equipment Grants Program (AET/SEGP) and Grand Challenges Canada. MJS acknowledges Mark McDermott for the use of the thermal evaporator.

References:

[1] I.C. Kwon, Y.H. Bae, S.W. Kim, Nature 354 (1991) 291.

[2] A. Suzuki, T. Tanaka, Nature 346 (1990) 345.

[3] A. Gutowska, Y.H. Bae, H.A. Jacobs, J. Feijen, S.W. Kim, Macromolecules 27 (1994) 4167.

[4] R. Pelton, Advances in Colloid and Interface Science 85 (2000) 1.

[5] T. Wang, D. Liu, C. Lian, S. Zheng, X. Liu, Z. Tong, Soft Matter 8 (2012) 774.

[6] K. Haraguchi, K. Murata, T. Takehisa, Macromolecules 45 (2012) 385.

[7] J. P. Gong, Soft Matter 6 (2010) 2583.

[8] R. Liu, A. H. Milani, T. J. Freemont, B. R. Saunders, Soft Matter 7 (2011) 4696.

[9] J. Hu, K. Hiwatashi, T. Kurokawa, S. M. Liang, Z. L. Wu, J. P. Gong, Macromolecules 44 (2011) 7775.

[10] J. C. Gaulding, M. H. Smith, J. S. Hyatt, A. Fernandez-Nieves, L. A. Lyon, Macromolecules 45 (2012) 39.

281 [11] E. Ayano, M. Karaki, T. Ishihara, H. Kanazawa, T. Okano, Colloids Surf. B 99 (2012) 67.

282 [12] M.A. Nash, J.N. Waitumbi, A.S. Hoffman, P. Yager, P.S. Stayton, ACS Nano 6 (2012)
283 6776.

284 [13] C.S. Thomas, L. Xu, B.D. Olsen, Biomacromolecules 13 (2012) 2781.

285 [14] A. Kundu, R.K. Layek, A.K. Nandi, J. Mater. Chem. 22 (2012) 8139.

286 [15] G. Nagarjuna, A. Kumar, A. Kokil, K.G. Jadhav, S. Yurt, J. Kumar, D. Venkataraman, J.
287 Mater. Chem. 21 (2011) 16597.

288 [16] N. Morimoto, X.-P. Qiu, F.M. Winnik, K. Akiyoshi, Macromolecules 41 (2008) 5985.

289 [17] T. Alizadeh, M.R. Ganjali, M. Zare, Analytica Chimica Acta 689 (2011) 52.

290 [18] A. Dedinaite, E. Thormann, G. Olanya, P.M. Claesson, B. Nystrom, A.L. Kjoniksen, K.Z.
291 Zhu, Soft Matter 6 (2010) 2489.

292 [19] V.V. Yashin, O. Kuksenok, A.C. Balazs, Prog. Polym. Sci. 35 (2010) 155.

293 [20] H. Ouyang, Z.H. Xia, J.A. Zhe, Microfluid Nanofluid 9 (2010) 915.

294 [21] E.S.M. Lee, B. Shuter, J. Chan, M.S.K. Chong, J. Ding, S.H. Teoh, O. Beuf, A. Briguet,
295 K.C. Tam, M. Choolani, S.C. Wang, Biomaterials 31 (2010) 3296.

296 [22] W. Fischer, M. A. Quadir, A. Barnard, D.K. Smith, R. Haag, Macromol. Biosci. 11 (2011)
297 1736.

298 [23] R. Palankar, A. G. Skirtach, O. Kreft, M. Bedard, G. B. Sukhorukov, H. Möhwald, G. B.
299 Sukhorukov, M. Winterhalter, S. Springer, Small 19 (2009) 2168.

300 [24] E. Ayano, H. Kanazawa, J. Sep. Sci. 29 (2006) 738.

301 [25] H. Kanazawa, T. Okano, J. Chromatogr. A 1218 (2011) 8738.

302 [26] C.T. Black, K.W. Guarini, K.R. Milkove, S.M. Baker, T.P. Russell, M.T. Tuominen, Appl.
303 Phys. Lett. 79 (2001) 409.

304 [27] C.T. Black, K.W. Guarini, Y. Zhang, H. Kim, J. Benedict, E. Sikorski, I.V. Babich, K.R.
305 Milkove, IEEE Electron Device Lett. 25 (2004) 622.
306 [28] A.W. Bridges, N. Singh, K.L. Burns, J.E. Babensee, L.A. Lyon, A.J. Garcia, Biomaterials
307 29 (2008) 4605.
308 [29] X. Cai, C. Dong, H. Dong, G. Wang, G.M. Pauletti, X. Pan, H. Wen, I. Mehl, Y. Li, D. Shi,
309 Biomacromolecules 13 (2012) 1024.
310 [30] E.C. Cho, J. Lee, K. Cho, Macromolecules 36 (2003) 9929.
311 [31] O. Zavgorodnya, M.J. Serpe, Colloid. Polym. Sci. 289 (2011) 591.
312 [32] M.J. Serpe, L.A. Lyon, Chem. Mater. 16 (2004) 4373.
313 [33] K.C.C. Johnson, F. Mendez, M.J. Serpe, Anal. Chim. Acta 739 (2012) 83.
314 [34] R. Pelton, Adv. Colloid Interface Sci. 85 (2000) 1.
315 [35] X. Wu, R.H. Pelton, A.E. Hamielec, D.R. Woods, W. McPhee, Colloid. Polym. Sci. 272
316 (1994) 467.
317 [36] T. Hoare, R. Pelton, Macromolecules 37 (2004) 2544.
318 [37] K. Kratz, T. Hellweg, W. Eimer, Colloids Surf. A 170 (2000) 137.
319 [38] S. Zhou, B. Chu, J. Phys. Chem. B 102 (1998) 1364.
320 [39] A. Burmistrova, K.R. von, J. Mater. Chem. 20 (2010) 3502.
321 [40] S. Schmidt, T. Hellweg, K.R. von, Langmuir 24 (2008) 12595.
322 [41] M.C.D. Carter, C.D. Sorrell, M.J. Serpe, J. Phys. Chem. B 115 (2011) 14359.
323 [42] C.D. Sorrell, M.C.D. Carter, M.J. Serpe, Adv. Funct. Mater. 21 (2011) 425.
324 [43] C.D. Sorrell, M.J. Serpe, Adv. Mater. 23 (2011) 4088.
325 [44] C.D. Sorrell, M.C.D. Carter, M.J. Serpe, ACS Appl. Mater. Interfaces 3 (2011) 1140.
326 [45] K.K. Kanazawa, J.G. Gordon, Anal. Chim. Acta 175 (1985) 99.

327 [46] M.D. Ward, D.A. Buttry, Science 249 (1990) 1000.

328